UC San Diego

UC San Diego Previously Published Works

Title

Temporal-spatial structures of plasmas flows and turbulence around tearing mode islands in the edge tokamak plasmas

Permalink

Journal

ISSN

Authors

Zhao, KJ
Nagashima, Y
Li, FM
et al.

Publication Date

DOI

Copyright Information

Peer reviewed

Temporal-spatial structures of plasmas flows and turbulence around tearing mode islands in the edge tokamak plasmas

K. J. Zhao[1, 2], Y. Nagashima[3], F. M. Li[2], Yuejiang. Shi[4], P. H. Diamond[5], J. Q. Dong[1,8], K. Itoh[3, 6,7], S.- I. Itoh[3], G. Zhuang,[2] H. Liu,[2] Z. P. Chen,[2] J. Cheng,[1] L. Nie,[1] Y. H. Ding,[2] Q. M. Hu[2], Z. Y. Chen,[2] B. Rao,[2] Z. F. Cheng,[2] L. Gao,[2] X. Q. Zhang,[2] Z. J. Yang,[2] N. C. Wang,[2] L. Wang,[2] W. Jin,[2] W.Yan,[2] J. Q. Xu,[1] Y. F. Wu,[1] L. W. Yan,[1] A. Fujisawa[3], S. Inagaki[3], Y. Kosuga[3], M. Sasaki[3], and J-TEXT team[2]

1. *Southwestern Institute of Physics, P. O. Box 432, Chengdu, China*
2. *College of Electrical and Electronic Engineering, Huazhong University of Science and Technology, Wuhan Hubei, 430074, China*
3. *Research Institute for Applied Mechanics, Kyushu University, Kasuga, Kasuga koen 6-1, 816-8580, Japan*
4. *Department of Nuclear Engineering, Seoul National University, Seoul, Korea*
5. *Center for Momentum Transport and Flow Organization, University of California at San Diego, California 92093, USA*
6. *Institute of Science and Technology Research, Chubu University, Kasugai, Aichi, 487-8501 Japan*
7. *National Institute for Fusion Science, Toki 509-5292, Japan,*
8. *Institute for Fusion Theory and Simulation, Zhejiang University, Hangzhou, China*

Emails: kjzhao@swip.ac.cn and yjshi@ipp.ac.cn

The temporal-spatial structures of plasma flows and turbulence around tearing mode islands are presented. The experiments were performed using Langmuir probe arrays in the edge plasmas of J-TEXT tokamak. The correlation analyses clearly show that the flows have similar structures of m/n=3/1 as the magnetic island does (m and n are the poloidal and toroidal mode numbers, respectively). The sign of the potential fluctuations for the flows inverses and the powers significantly reduce at q=3 surface. Approaching to the last closed flux surface for the magnetic islands, the radially

elongated flow structure forms. The flows are concentrated near separatrix and show quadrupole structures. The turbulence is concentrated near X-point and partly trapped inside the magnetic islands.

PACS numbers: 52. 35. Ra, 52. 25. Fi, 52. 35. Mw, 52. 55. Fa

1. Introduction

Interaction of magnetic field structures and flows in magnetohydrodynamics is a subject of general interest in physics. Typical examples include magnetic braking of stellar rotation [1], angular momentum transport in astrophysical disks [2, 3], and dynamics of the earth core and geodynamo [4]. In fusion plasmas, the interactions between plasma flows and magnetic fluctuations have attracted attentions for understanding and control of plasma confinement and transport [5-9]. For example, the neoclassical tearing modes (NTMs), which need a seed magnetic island for onset [10, 11], can be, theoretically, triggered by a turbulence noise source [12]. At the same time, the magnetic island-induced sheared flows can suppress turbulence and contribute to the formation of an internal transport barrier [13]. For the mitigation/suppression of the large edge localized modes (ELMs) in the H-mode plasmas, which is considered to be an urgent task for fusion researches, the resonant magnetic perturbations (RMPs) [14] are used worldwide. In applying RMPs, the interactions of magnetic perturbations, zonal flows [15-16], and microscopic turbulence take place.

The RMP-induced magnetic islands have been studied extensively. The poloidal flows are reversed when the RMP-induced island width is large enough [17]. The static island can enhance the low frequency flows and turbulence at their boundaries [18-19]. The turbulence is weak inside magnetic islands that is consistent with the observations of low gradient of electron temperature [20], and reduced electron thermal conductivity [21]. The NTM-induced islands modulate density fluctuations in the core plasmas [22]. Synchronization of magnetic islands and geodesic acoustic modes (GAMs), a new mechanism of coherent structure formation is found in the edge tokamak plasmas [23-24]. Although the importance of mutual interaction between turbulent fluctuations and

magnetic islands has been widely recognized, quadrupole structures of the flows and the radially elongated flow formation in the vicinity of magnetic islands have not been reported.

To understand the complicated interaction of plasma flows with magnetic islands, the spatial and temporal structures of plasma flows and turbulence around magnetic islands should be tested experimentally. Here，the first observation of the quadrupole structures of the flows and the turbulence near the X-point are consistent with the theoretical expectation [10]. The discovery of
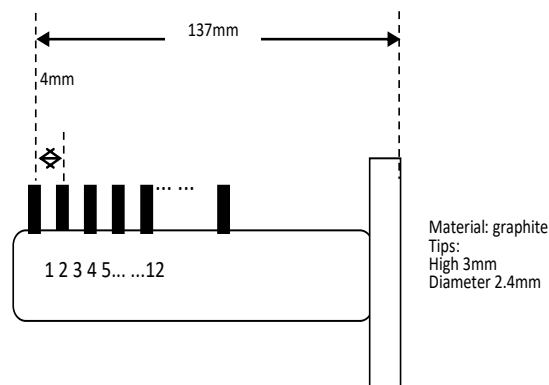

Fig.1 The configuration of the radial rake Langmuir probe array.

the radially elongated flows due to magnetic islands suggests that there might be various mechanisms of the flows interacting with magnetic islands in the high temperature plasmas.

The rest of this work is organized as follows. The experimental set-up is given in section 2. The experimental results, described in section 3, include the observation of tearing modes and their associated potential perturbations, the flow structure around tearing mode islands, the temporal-spatial structures of flows and turbulence with magnetic islands, turbulence envelope modulation by magnetic islands, the radial profiles of flows and turbulence, the radial dependences of the plasma parameters with tearing mode islands, etc. Section 4 presents the conclusion and discussion.

2. Experiment setup

The experiments presented here were conducted in Ohmic plasmas of a circular cross section on the J-TEXT tokamak. The major and minor radii of the machine are R = 1.05 m and a = 0.255 m, respectively. The parameters specially set for the experiments are the toroidal magnetic field $B_t = 1.5 - 1.6 T$, the plasma current $I_p = 140 - 160 kA$,

the line averaged electron density $N_e = 1 - 2 \times 10^{19} \, m^{-3}$, and the edge safety factor q_a=3.2

- 3.5. The sampling rate of the probe data is 2 MHz corresponding to Nyquist frequency

of 1MHz. A radial rake probe array of 12 tips was used to get the profiles of the floating

potentials and the radial electric field, as shown in Figure 1. The tip size and the mount

of the LP sets are the same as was described in Ref. [18]. The probe array was installed

at the top of the device.

3. Experiment results

3.1 Observations of m/n=3/1 potential fluctuations and tearing modes

The m/n=3/1 potential fluctuations are detected inside the last closed flux surface

(LCFS). Figure 2(a) gives the auto-power spectra of the floating potential fluctuations at the positions of $\Delta r = -0.9$ cm, where the minus sign means inwards from the LCFS. A significant peak with the frequency of ~10 kHz is the m/n=3/1 potential fluctuation. Another peak at the frequency of ~18 kHz has been identified as geodesic acoustic modes [25-26].
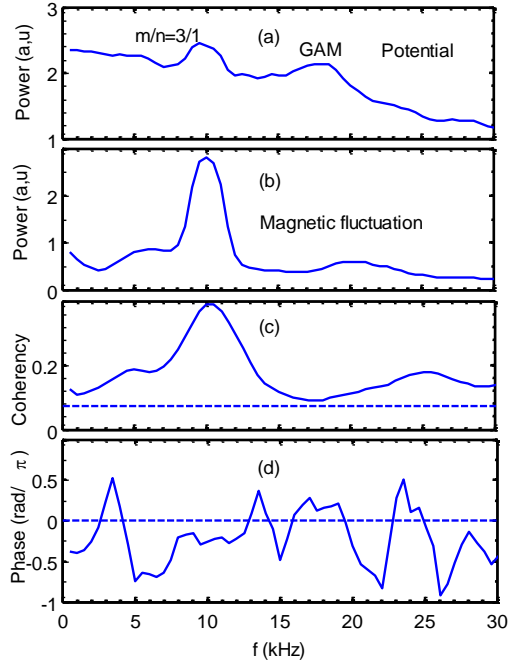

Fig 2 Auto-power spectra of floating potential fluctuations (a) and magnetic fluctuations (b), coherencies between magnetic fluctuations and floating potential fluctuations (c), and their phase shifts (d). (shot: 1034413).

Figure 2 (b) presents the auto power spectra of the magnetic fluctuations from the Mirnov coils set up on the vacuum vessel wall. The large peak at the frequency of ~10 kHz is the

tearing mode of m/n=3/1 [27]. The correlation between m/n=3/1 potential fluctuations

and magnetic fluctuations is evaluated by the fast Fourier transform (FFT) as shown in

the Figure 2 (c). The calculated coherencies at the frequency of ~10 kHz are

significantly above the noise level, indicating that the m/n=3/1 potential fluctuations are well correlated with the m/n=3/1 magnetic islands. The phase shifts between potential fluctuations and magnetic fluctuations are described in Figure 2 (d). The phase shift is finite and depends on the Mirnov coil and Langmuir probe positions due to the spatial periodicity of the islands and flows. The poloidal (toroidal) velocity of the islands is estimated as 5km/s (20km/s).

The spatial structures of the m/n=3/1 tearing modes are analyzed from the Mirnov signals. The δB_r and δB_θ from poloidal Mirnov coils are shown in Figure 3(a). Here, δB_r and δB_θ are the radial and poloidal components of magnetic perturbations, respectively. Based on the values of δB_r and δB_θ, the poloidal mode number of m=3 is determined. Similarly, the toroidal mode number of n=1 is obtained, as shown in Figure 3(b).
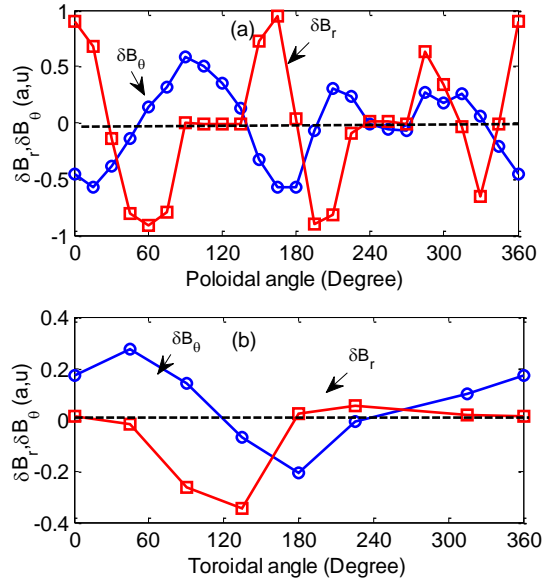

Fig. 3 The amplitudes of the radial and poloidal components for magnetic fluctuations from poloidal Mirnov coils (a), and from toroidal Mirnov coils (b). (Shot: 1034413).

3.2 Spatial structures of m/n=3/1 flows

The poloidal structure of the flows at the frequency of ~10 kHz was identified in the radial-poloidal plane with long range correlation analysis method. The coherency is defined as $C_{XY} = \langle (X_i - X)(Y_i - Y) \rangle / [\sqrt{< (X_i - X)^2 >} \sqrt{< (Y_i - Y)^2 >}]$, where X_i and Y_i are two sets of variables, *i* stands for time series, and N is an integer. The value of coherency is from -1 to 1 and can be used to detect the periodical structure. Figure 4 (a) shows the contour plot of the coherency $C(X(\Delta r), Y(\zeta))$ at q_a=3.5 for shot 1034410, where $X(\Delta r)$

5

is the potential perturbation at r = a+ Δr and Y(ζ) is $d\tilde{b}_\theta/dt$ at the poloidal angle ζ.

The 12 probe tips are uniformly distributed in the radial direction from -2.9 to 1.5 cm. The 24 Mirnov coils are located at different poloidal positions uniformly. The poloidal mode number of the potential fluctuation at the frequency of ~10 kHz is clearly demonstrated as m=3. The potential
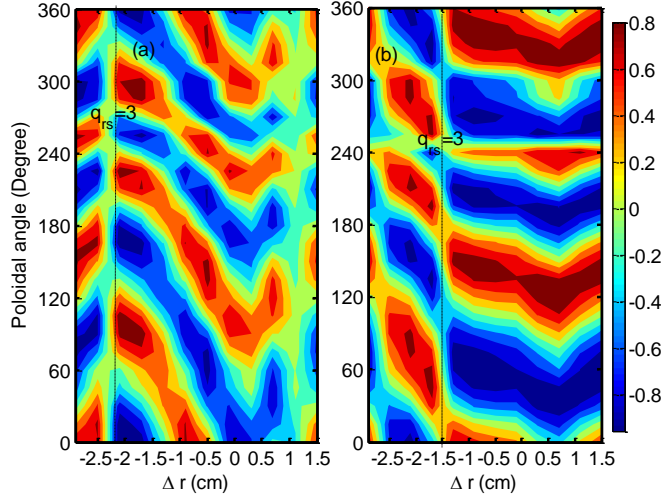

Fig. 4 The contours of coherency between potentials and poloidal magnetic fluctuations (a) at q_a=3.5 and (b) at q_a=3.2.

fluctuation propagates in the electron diamagnetic drift direction. The radial wave length of the m=3 flow is ~1.5cm. The q=3 surface (dashed line) can be evaluated from

the magnetic measurements and is consistent with the estimations from the sign of the potentials. For comparison, the contour plot of the coherency C(X(Δr), Y(ζ)) at q_a=3.2 is provided in Figure 4(b) for shot 1034413. Similarly, the mode number of the flow is m=3. Note that the m=3 flows are elongated near the LCFS in the radial direction in this case.
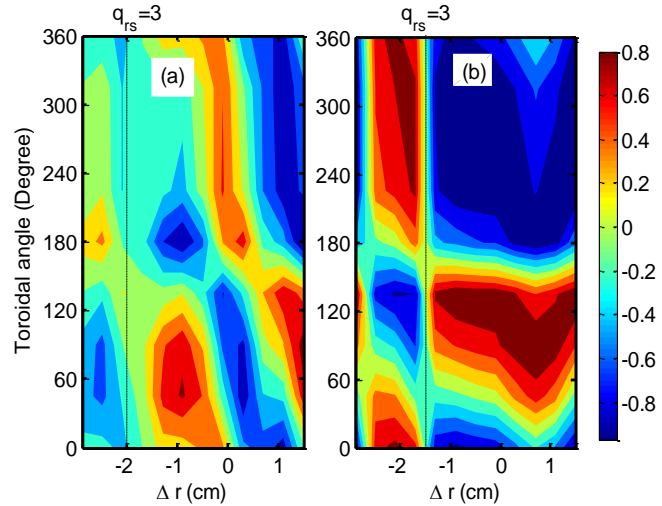

Fig. 5 The contours of coherency between potentials and toroidal magnetic fluctuations (a) at q_a=3.5 and (b) at q_a=3.2.

This differs from the cases at q_a=3.5, where the flows are elongated in the poloidal direction. Based on the significant difference of the flow structures at q_a=3.5 and q_a=3.2,

we infer that there might be various mechanisms of the magnetic island interacting with the flows. At q_a=3.5, it can be considered as that tearing mode is simply interacting with turbulence because the island is far away from the LCFS. However, other effects may also be included at q_a=3.2 in the radial structure formation owing closing to the LCFS.

The structure in the radial-toroidal plane of the flows at the frequency of ~10 kHz was also obtained, using correlation analysis technique. Figure 5 (a) gives the contour plot of the coherency between potentials and magnetic fluctuations in the frequency bands of 9-11 kHz at q_a=3.5. The 8 Mirnov coils are distributed uniformly in the toroidal direction. The toroidal mode number of n=1 is demonstrated apparently. This result indicates that the flows at ~10 kHz have a clear structure of m/n=3/1 mode. The flow propagation direction is opposite to the toroidal magnetic field. The flows are also elongated radially near the LCFS at q_a=3.2, as given in the figure 5 (b).

3.3 Turbulence envelope modulation

The radial and toroidal structures for the turbulence envelope in the frequency bands of 9-11 kHz at q_a=3.5 and 3.2 are provided in Figures 6(a) and (b), respectively. The edge turbulence moves in the electron diamagnetic direction and the radial correlation length is ~1cm. Thus, it might be trapped electron mode. Here, the turbulence envelope is similar to

Fig. 6 The contours of coherency between turbulence envelopes and magnetic fluctuations from toroidal Mirnov coils at q_a=3.5 (a) and 3.2 (b).

the turbulence intensity. It is calculated from the high frequency fluctuations of 30 -150 kHz with Hilbert transform. The envelope can be described as $\sqrt{x_{(t)}^2 + y_{(t)}^2}$, where, $x_{(t)}$ and $y_{(t)}$ are the real and imaginary parts of the analytic signal, respectively [28].
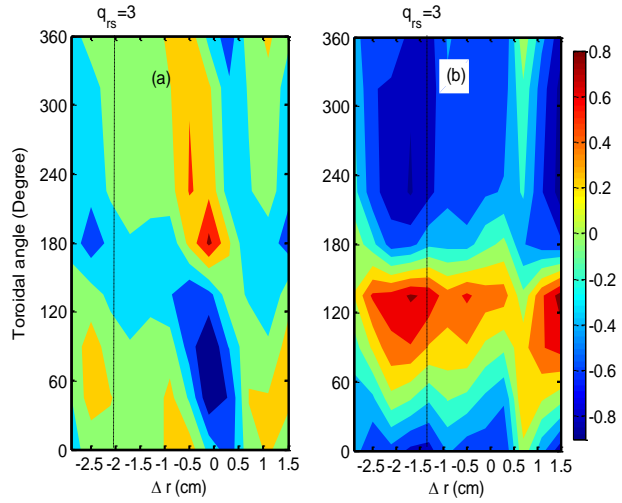
The toroidal （poloidal）mode numbers for the turbulence envelope are identified as n=1 (m=3) in both cases. At q_a=3.5 (q_a=3.2), the turbulence envelope is also elongated in the toroidal (radial) direction and are consistent with the mode structures of the m/n=3/1 flows. This observation suggests that magnetic islands modulate turbulence.

3.4 Temporal-spatial structures of m/n=3/1 potential fluctuations and turbulence envelopes

The spatio-temporal distributions of the m/n=3/1 potential fluctuations and the turbulence envelopes are presented in Figures 7(a) and (b) at q_a=3.2, respectively. Here, the magnetic islands are indicated with the dashed curves. The change of the sign for the m/n=3/1 electrostatic potentials at $\Delta r = -1.5cm$ is clearly shown. The horizontal-dashed lines indicate the position of q=3 surface. The island width is calculated as $w \sim \delta B_r^{1/2}$ ~1.5cm from the magnetic measurements. Considering that the flows are toward the X-points [1], the X-points and O-points of magnetic islands can be identified from the sign of

Fig. 7 The contours of m/n=3/1 potential fluctuations (a) and turbulence envelope in the island frequency bands (b), turbulence intensity (c), and turbulence envelope in the island frequency bands (d) at q_a=3.2 (the magnetic islands are indicated by the dashed curves).

potential fluctuations. Based on the measurements of the q=3 surface, island width and X-points, and assuming the 'separatrix' is satisfied with a sine or cosine function, the location of the magnetic islands is evaluated. The flows are concentrated near the separatrix and have quadrupole structures. The measurements are in good agreement
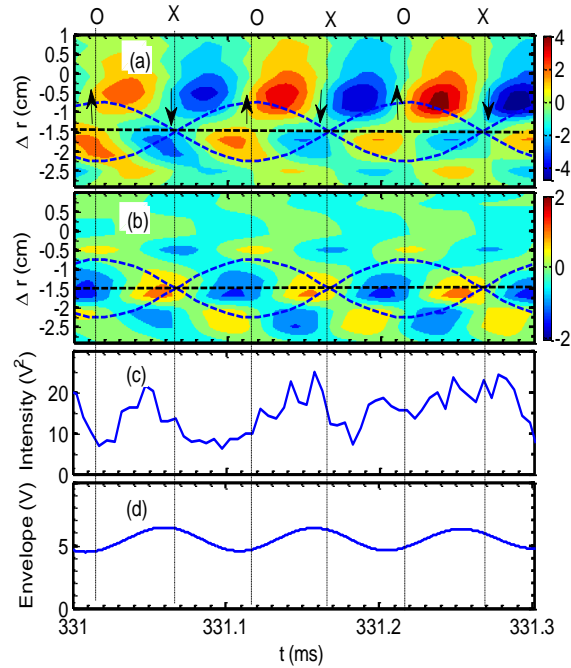
with the prediction of theory [10]. The turbulence is concentrated near the X-points and partly trapped inside the islands (Fig. 7(b)).　　For understanding of the island effects on turbulence, Figure 7 (c) gives the time evolutions of the turbulence intensity $\delta\phi_f^2$ in the frequency bands of 30-150 kHz at the position of $\Delta r = -1.5 cm$. The higher turbulence intensity near the X-point also suggests magnetic islands modulation on turbulence [8-9, 29-34]. The amplitudes of the turbulence envelopes in the frequency bands of 9-11 kHz at the same position are provided in Figure 7 (d). The modulation of magnetic island on turbulence is clearly shown again. In addition, the island width is estimated as ~1.5cm at q_a=3.5.

3.5 Radial profiles of the turbulence and m/n=3/1 potential fluctuations

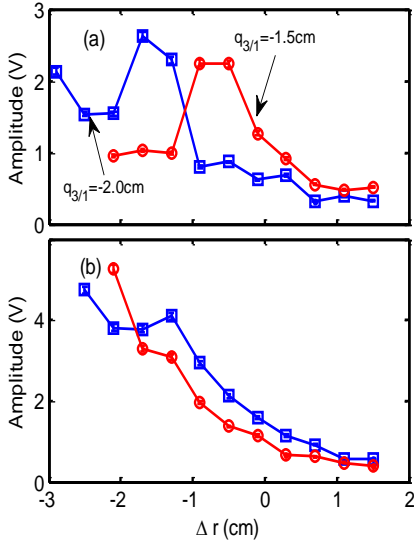To understand the effects of islands on turbulence, the radial

Fig. 8 The radial distributions of turbulence intensity during X-point and O-point phases, and for a long-time average.

Fig. 9 The radial distributions of the amplitudes of the m/n=3/1 potential fluctuation (a) and averaged turbulence (b).
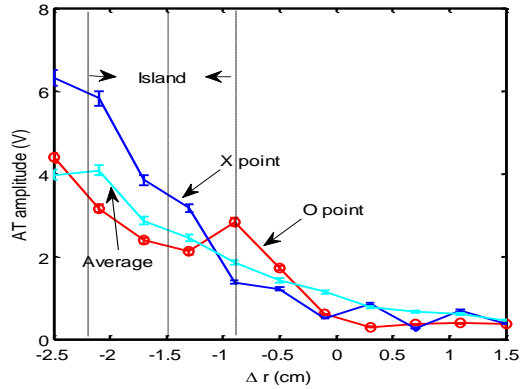
profiles of the turbulence amplitudes are studied further. Figure. 8 shows the radial distributions of turbulence amplitudes during X-point and O-point phases, and for a long-time average. The turbulence amplitudes are calculated by $\left|\delta\phi_f\right|$ from the high frequency part of 30-150 kHz. In the region of Δr ~-2.1 to ~-1.2 cm, the turbulence amplitudes are lower and higher than the mean

turbulence amplitudes during O-point and X-point phases, respectively. This result suggests that turbulence is concentrated near X-points again. At the outer boundary of the islands, the turbulence amplitude is higher during O-point phase.

The profiles of the flows and turbulence are investigated via varying the edge safety factor. Figure 9 (a) describes the radial profiles of the amplitudes for the m/n=3/1 modes at q_a=3.2 and 3.5. The position of q=3 surfaces is ~-2.0 cm for q_a=3.5. The amplitudes of the m/n=3/1 modes drop inside the islands and is higher at the island boundaries. The peak of the m/n=3/1 mode amplitudes moves outward at q_a=3.2 so that the m/n=3/1 mode has higher intensity near the LCFS. The radial distributions of the turbulence amplitudes are given in Figure 9 (b). At q_a=3.5, the turbulence amplitudes are lower (higher) inside the magnetic islands (at the island boundaries). The shape of the radial profiles for the turbulence amplitudes are much different at q_a=3.2. The turbulence amplitude increases inward while the peak at the outer boundary of the islands disappears. This is consistent with the cases of static islands, i.e, the turbulence intensity drops near the LCFS with static islands [18].

4. Conclusion and discussion

The temporal-spatial structures of plasma flow and turbulence in the vicinity of tearing mode islands are studied. The experiments were performed using Langmuir probe arrays in the edge plasmas of the J-TEXT tokamak. Some common features are obtained. The correlation analyses between potential and magnetic fluctuations clearly show that the flows have similar structures of m/n=3/1 as the magnetic island does. The sign of the potential fluctuations for the flows inverses and the powers significantly reduce at q=3 surface. The results are consistent with the cases of RMPs. The flows are elongated in the poloidal and toroidal directions. When the magnetic islands approach to the LCFS, the flow structure changes significantly and are elongated in the radial direction.

Approaching to the LCFS, i.e., at q_a=3.2, the temporal-spatial structures of plasma flow and turbulence are also demonstrated. The flows are concentrated along separatrix and show quadrupole structures. The turbulence is concentrated near X-point and partly

trapped inside the magnetic islands.

Note that the flow structure around magnetic islands depend on the locations of the magnetic islands. However, the spatio-temporal structures of the plasma flows and turbulence are only obtained at $q_a=3.2$. For better understanding of the interaction between magnetic islands and flows, the spatio-temporal structures of the plasma flow and turbulence should also be detected in deeper plasmas and its dependence on the island widths should also be tested experimentally.

The impact of turbulence on the growth of the island is important and interesting. However, the turbulence information is just available during the saturation phase of the magnetic islands because the nonlinear growth of the islands is too fast. To understand the turbulence effects on the growth of the island, the diagnostics for measuring the turbulence during the growing phase of the islands is still a challenge.

The stability parameter of tearing mode is another important parameter which is not estimated due to the lack of measurements. However, normally, the observed MHD instability is a tearing mode in Ohmic edge plasmas. In addition, the poloidal and toroidal velocities of the islands close to the plasma rotation velocities.

It is well known that the edge flows play an important role in plasma confinement and transport. Thus, the changes of the flow structure around magnetic islands in the edge plasmas suggest that magnetic islands can be as a tool to control plasma confinement and transport.

[1] Matt Seanp, et al., APJ, **754**, L26 (2012).

[2] S. A. Balbus and J. F. Hawley, APJ, **376**, 241(1991).

[3] S. A. Balbus and J. F. Hawley, Rev. Mode. Phys, **70**, 1, (1998).

[4] J. Aubert and A. Fournier, Nonlin. Processes Geophys, **18**, 657(2011).

[5] J. L. Wang et al., Nucl. Fusion 57, 046007 (2017).

[6] Z.Q. Hu, et al., Nucl. Fusion 56, 016012 (2016).

[7] Z.Q. Hu et al., Nucl. Fusion 54, 123018 (2014).

[8] A. Ishizawa and N. Nakajima, Physics of Plasmas 14, 040702 (2007)

[9] A. Ishizawa and N. Nakajima, Nuclear Fusion 49, 055015 (2009)

[10] D. Biskamp, Magnetic Reconnection in Plasmas, (Cambridge University Press, Cambridge, England, 2000).

[11] P. K. Kaw, E. J. Valeo, and P. H. Rutherford, Phys. Rev.Lett. 43, 1398 (1979).

[12] S-I. Itoh, K. Itoh, and M. Yagi, Phys. Rev. Lett. 91, 045003 (2003).

[13] T. Estrada et al, Nucl. Fusion, 47, 305 (2007).

[14] T. E. Evans et al., Phys. Rev. Lett. 92, 235003 (2004).

[15] A. Hasegawa and M. Wakatani et al., Phys. Rev. Lett. 59, 1581 (1987).

[16] P. H. Diamond et al., Plasma Phys. Cont. Fusion 47, R35 (2005).

[17] K. Ida, et al., Phys. Rev. Lett. 88, 015002 (2001).

[18] K. J. Zhao et al., Nucl. Fusion 55, 073022 (2015).

[19] K. J. Zhao et al., Nucl. Fusion 56, 076005 (2016).

[20] W. Suttrop et al., Nucl. Fusion, 37, 119 (1997).

[21] S. Inagaki et al., Phys. Rev. Lett. 92**,** 055002 (2004).

[22] L. Bardóczi et al., Phys. Rev. Lett. 116, 215001 (2016).

[23] K. J. Zhao et al., Phys. Rev. Lett. 117, 145002(2016).

[24] K. J. Zhao et al., Nucl. Fusion 57, 076036 (2017).

[25] K. J. Zhao et al., Phys. Rev. Lett. 95, 255004(2006).

[26] K. J. Zhao et al., Plasma Phys. Cont. Fusion, 52, 124008(2010).

[27] P. H. Rutherford, Phys. Fluids, 16,1903(1973).

[28] R. Jha, D. Raju and A. Sen, Phys. Plasmas, 13,082507 (2006).

[29] W. A. Hornsby et al., Phys. Plamas 17, 092301 (2010).

[30] W. A. Hornsby et al., Plasma Phys. Controlled Fusion 57, 054018 (2015).

[31] O. Izacard et al., Phys. Plasmas 23, 022304 (2016).

[32] D. Zarzoso et al., Nucl. Fusion 55 113018(2015).

[33] P. Hill, F. Hariri, and M. Ottaviani, Phys. Plasmas 22, 042308 (2015).

[34] A. Banon Navarro et al., Plasma Phys. Controlled Fusion 59, 034004 (2017).